

[Article ID] 1003- 6326(2002) 02- 0214- 04

Evolution of Ti(C, N)-based cermet microstructures^①

LI Chenhui(李晨辉), XIONG Weihao(熊惟皓), YU Lixin(余立新)

(State Key Laboratory of Die and Mould Technology, College of Materials Science and Engineering, Huazhong University of Science and Technology, Wuhan 430074, China)

[Abstract] Two series of Ti(C, N)-based cermet materials originating from the same chemical composition but with different grain size distribution and sintered to different stages of the sintering cycle have been studied using SEM, TEM, EDX, and XRD. Much of the surrounding structure is formed during solid state sintering. During the solid state sintering, at first, the Mo and W rich (Ti, Mo, W)C inner rim is formed by the interaction among TiC, WC, and Mo₂C; then the Mo and W lean (Ti, Mo, W)(C, N) outer rim is formed. During the liquid phase sintering, the outer rim of coarse grains grows rapidly through a solution-precipitation process; also coarse grains grow by particle coalescence. The interface between coarse grain outer rim and binder is flat (crystal surface).

[Key words] Ti(C, N); cermet; microstructure

[CLC number] TF 125.3

[Document code] A

1 INTRODUCTION

Ti(C, N)-based cermets consist mainly of hard carbonitride grains, hereafter we call it as hard grain, embedded in a tough binder phase that is based on Co or Ni^[1]. Cermets usually contain Mo₂C or WC to improve wetting of the carbonitride grains by the binder^[2]. Most of the carbonitride particles have core-rim structure. The formation mechanism of this delicate structure is not yet clearly understood. Suzuki et al^[3] proposed the dissolution of Mo₂C and TiC particles into liquid Ni and reprecipitation of (Ti, Mo)C on large particles to form the surrounding structure. Ahn et al^[4] and Chun et al^[5] suggested the same core-rim formation mechanism in Ti-Mo-Ni and Ti(C, N)-WC-Ni cermets respectively. But Yang et al^[6] suggested that (Mo, Ti)(C, N) be formed by the solid diffusion of Ti from neighboring Ti(C, N) particles to Mo, then the rim structure be formed by dissolution of Ti(C, N) and (Mo, Ti)(C, N) particles into liquid binder phase and reprecipitation onto large Ti(C, N) particles. For the microstructure is the first most important determinant of cermets mechanical properties, a detailed research on the microstructure evolution of cermets during sintering is very important for promoting thoroughly understanding core-rim structure forming mechanism and improving mechanical properties of cermets.

2 EXPERIMENTAL

Two powder mixtures with the same composition

of TiC-10TiN-6.5WC-17Mo-1.7C-25Ni (mass fraction, %) were prepared by milling for 24 h, and then cold pressed into green compacts. One of them is a submicron powder mixture, and the other is a micron powder mixture. The sintering for X-ray diffraction (XRD) samples was interrupted at different stages of the sintering process (Fig. 1). Samples for scanning electron microscopy (SEM) and transmission electron microscopy (TEM) were prepared by a sinter-HIP

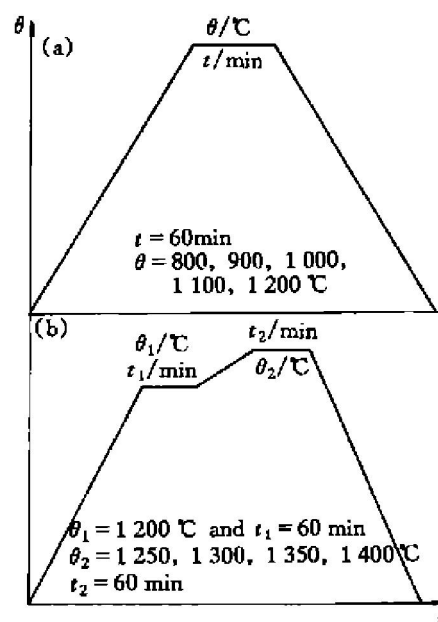


Fig. 1 Sintering process for XRD experimental samples

(a) —Process of samples sintered at 1200 °C or below;
(b) —Process of samples sintered at 1250 °C or above

① **[Foundation item]** Project (50074017) supported by the National Natural Science Foundation of China; project (1999048714) supported by the National Doctorate Program Fund of Education Ministry of China; project (992P0332) supported by Key Science and Technology Development Foundation of Hubei Province; project (67- 39) supported by State Key Lab for Powder Metallurgy and project supported by State Key Lab for Laser Technology **[Received date]** 2001- 07- 24; **[Accepted date]** 2001- 10- 17

process at 1420 °C^[7].

The microstructure of cermets was studied by a JSM-5600LV SEM with a Noran Vantage 4015 EDX system (element detection range from ${}_{5}\text{B}$ - ${}_{92}\text{U}$). The orientation relationship either between hard grain and neighboring binder or between two neighboring hard grains was studied by H-800 TEM selected area electron diffraction (SAED), and elemental distribution in cermets was studied by H-800 TEM PV9100/70 EDX (element detection range from ${}_{11}\text{Na}$ - ${}_{92}\text{U}$). Sintered samples were crushed into less than 74 μm particles and monitored by X-ray diffraction to determine the phase transformation during sintering. The relative intensity of $\text{Ti}(\text{C}_x, \text{N}_{1-x})$ (111), Ni (111), graphite (002), WC (100), Mo (110), Mo_2C (101), TiN (200), $(\text{W}, \text{Ti})\text{C}_{1-x}$ (200) vs the total intensity of afore mentioned diffraction peaks was calculated to indicate the relative concentration change of different phases during sintering. The lattice parameters of the main phases occurring during sintering were calculated from the measured d -spacing data derived from X-ray powder diffraction peaks.

3 RESULTS AND DISCUSSION

The microstructures of Ti(C, N)-based cermet are shown in Fig. 2. Hard phase grains have an obvious double layers surrounding structure, in which the

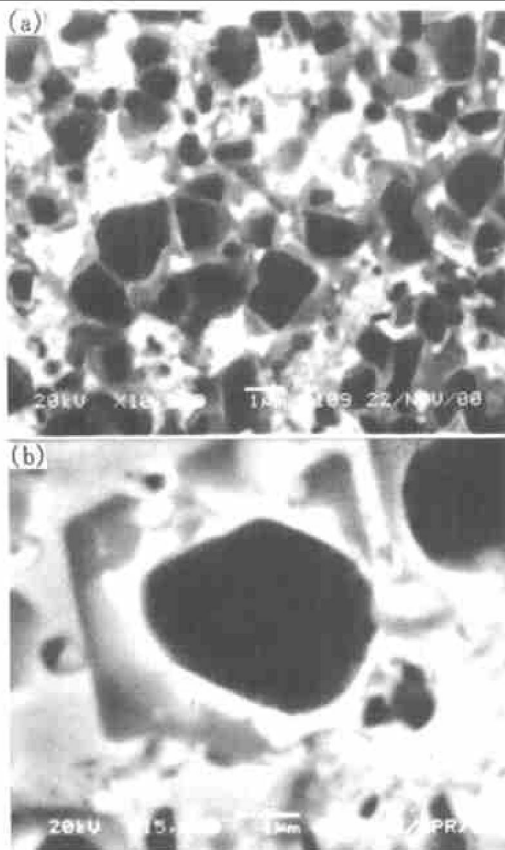


Fig. 2 Scanning electron micrographs of normal cermet (BSE)
(a) —General view; (b) —Surrounding structure and interface condition of coarse grain

inner rim has the highest average atomic number among core, inner rim, and outer rim, and its thickness is uneven; however, the outer rim has a average atomic number between core and inner rim, and it is much thicker than inner rim. The interface between coarse hard grain and binder is flat (crystal surface). Particle coalescence through neck growth was observed between coarse hard grains and neighboring fine hard grains. The flat interface between hard grain and binder indicates that the growth of outer rim through binder is controlled by interface reaction, which is consistent with Refs. [8, 9].

The STEM/EDX analyses of typical core-“inner-rim”-“outer-rim” surrounding structure show that the core is consisted of almost pure TiC; however, the content of Mo or W is quite high in rim, and their contents in inner-rim are much higher than their contents in outer-rim (Fig. 3). SAED analyses indicate that there is no constant orientation relationship between hard grain and neighboring binder or between two neighboring hard grains^[10~12]; however, in this research, the same orientation relationship do exists between hard grain and neighboring binder whose interface is flat (crystal surface), or between a coarse hard grain and a neighboring small hard grain. The orientation relationship may be expressed as $(hkl)_{\text{Ti}(\text{C}, \text{N})} \parallel (hkl)_{\text{Ni}}$, and $(hkl)_{\text{Ti}(\text{C}, \text{N})} \parallel (hkl)_{\text{Ti}(\text{C}, \text{N})}$. The first type of parallel orientation relationship indicates that the binder can nucleate heterogeneously using the hard grains as substrates during solidification. Both binder and hard grains have a FCC structure, so they keep the same orientation relationship to help reducing interface energy and nucleation. The second type of parallel orientation relationship indicates that neighboring hard grains keep the same orientation relationship through particle rearrangement to help coalescence during sintering. Usually, small particles are easily to adjust themselves' angle to keep the same orientation with neighboring coarse grains; nevertheless, the rearrangement of coarse grains is restricted by neighboring particles and needs more energy, so two neighboring coarse grains rarely have the same orientation relationship.

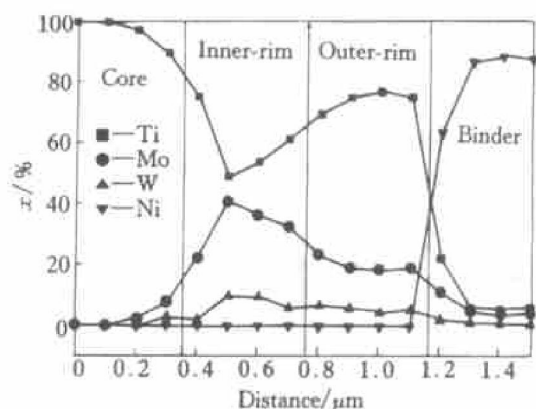


Fig. 3 Element distributions in cermet

Phase transformations of submicron cermet during sintering are shown in Fig. 4. Here the interplanar spacings of hard grain and binder change with the variety of sintering temperature, and the width of diffraction peaks broadens out rapidly at 1100 °C. The reaction of $2\text{Mo} + \text{C} \rightarrow \text{Mo}_2\text{C}$ can be finished at 800 °C, and it causes the disappearance of Mo. WC and Mo_2C disappear at 1200 °C, and TiN disappears at 1250 °C. The relative intensity of the main phases are shown in Fig. 5, which shows that the concentration of hard grain phase increases rapidly at 1100~1250 °C. That the concentration of hard grain phase increases with decreasing WC and Mo_2C concentration at 1100 °C and 1200 °C indicates the formation of (Ti, Mo, W)C inner-rim. Because both (Ti, Mo, W)C and (Ti, Mo, W)(C, N) have the same FCC structure as TiC, and the varieties of lattice parameters among them are almost negligible^[13], the respective diffraction peaks of (Ti, Mo, W)C or (Ti, Mo, W)(C, N) can not be seen, but it is obvious that the width of TiC diffraction peaks broadens out rapidly (Fig. 4), and the relative intensity of them increases rapidly (Fig. 5). Taking into account the atomic radii of the atoms contained in this cermet, which is Ti (1.4318 Å) > W (1.3705 Å) > Mo (1.3626 Å) > Ni (1.2458 Å) > C (0.77 Å) > N (0.75 Å)^[14], the lattice constant of (Ti, Mo, W)(C, N) decreases with increasing Mo, W (W and Mo occupy some of titanium sites in the lattice) and N (N atoms occupy some of C sites in the lattice) content; therefore, the formation of (Ti, Mo, W)C or (Ti, Mo, W)(C, N) causes a reduction of TiC lattice parameters without exception, and that is consistent with the changes of

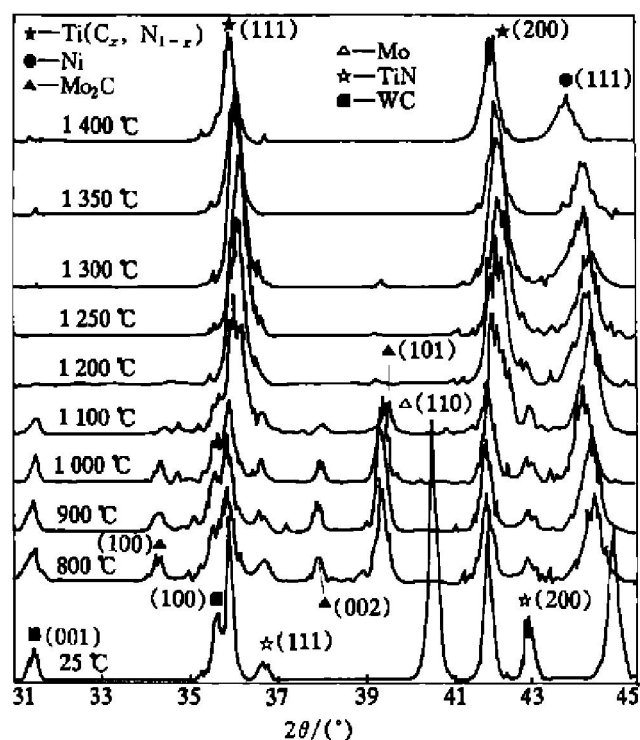


Fig. 4 Phase transformation of submicron cermet during sintering

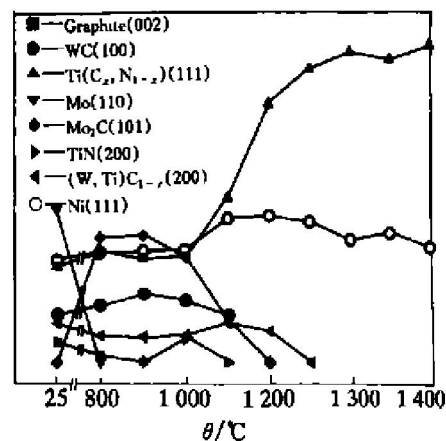


Fig. 5 Relative intensities of different phases in submicron cermet during sintering

experimental obtained lattice parameters. (That the lattice constant increases above 1250 °C is due to denitrification^[15] as shown in Fig. 4).

Through comparing Fig. 5 with Fig. 6, we can see that a change of powder particle size does not have an effect on sintering mechanism, but it does have an effect on sintering kinetics. That the general mutation trend of lattice parameters concerning to different particle size powder mixtures during sintering is almost the same (Fig. 7). As for sub-micron cermet, its TiC core homogenizes with inner-rim through diffusion during sintering for its small particle size, which causes the disappearance of inner-rim, and finally it shows a single layer surrounding structure after sintering. However, when the content of Mo_2C , WC, or TiN is very high, or their particle size is large, part of those powders will be reserved in cermet after sintering^[1].

Because the liquid phase is always formed above 1350 °C^[11,16], the surrounding structure of hard grain phase is mainly formed during solid state sintering process. The inner rim, formed during solid state sintering, is very unevenly distributed onto the Ti(C, N) grains (cores), which indicates that bulk dif-

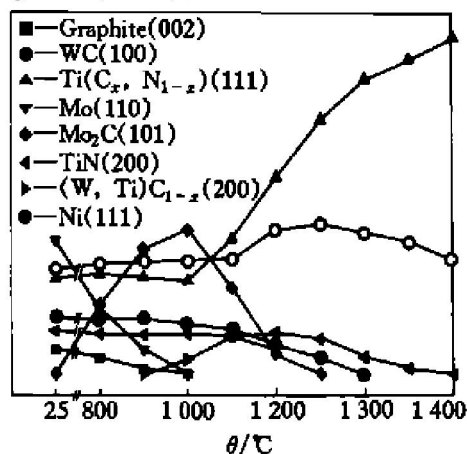


Fig. 6 Relative intensities of different phases in micron cermet during sintering

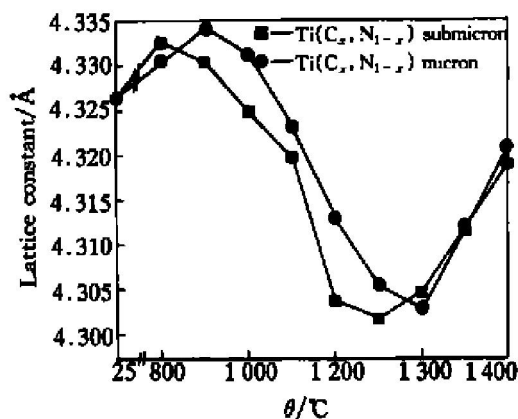


Fig. 7 Lattice constants of $\text{Ti}(\text{C}_x, \text{N}_{1-x})$ vs sintering temperature

fusion through the binder is the dominating transport path rather than surface diffusion (Fig. 2(b)). Because the solubility of a grain in its surrounding liquid varies inversely with the grain size, small grains dissolve in liquid and reprecipitate on neighboring coarse grains surface during the following liquid phase sintering process, and which causes grain coarsening. The other way of grain coarsening during liquid phase sintering is grain coalescence through a grain rearrangement, neck growth, and coalescence process. Both ways of grain coarsening can be seen in Fig. 2.

4 CONCLUSIONS

1) The core-rim structure of $\text{Ti}(\text{C}, \text{N})$ -based cermet is mainly formed during solid state sintering.

2) The core-rim microstructure forming process can be described as follows: during solid state sintering, at first, Mo and W rich $(\text{Ti}, \text{Mo}, \text{W})\text{C}$ inner rim is formed by the interaction among TiC , WC , and Mo_2C ; then Mo and W lean $(\text{Ti}, \text{Mo}, \text{W})(\text{C}, \text{N})$ outer rim is formed. During the liquid phase sintering, the outer rim of coarse grains grows rapidly through a solution-reprecipitation process; also coarse grains grow by particle coalescence.

3) The interface between coarse grain outer rim and binder, formed by solution-reprecipitation, is flat (crystal surface); however, the interface between hard grain and binder, formed by particle coalescence, is irregular.

[REFERENCES]

[1] Lindahl P, Gustafson P, Rolander U, et al. Microstruc-

- ture of model cermets with high Mo or W content [J]. *Int J RM & HM*, 1999, 17(3): 411– 421.
- [2] Doi H. Advanced TiC and TiC-TiN base cermets [A]. Almond E A, Brookes C A, Warren R. *Science of Hard Materials* [C]. Inst Phys Conf Ser No 75. Bristol: Adam Hilger, 1986. 489– 523.
- [3] Suzuki H, Hayashi K, Terada O. Two-phase region in TiC-Mo-30Ni alloys [J]. *J Jpn Inst Metals*, 1971. 35 (2): 146– 150.
- [4] Ahn S Y, Kang S. Formation of core/rim structures in $\text{Ti}(\text{C}, \text{N})\text{-WC-Ni}$ cermets via a dissolution and precipitation process [J]. *J Am Cer Soc*, 2000, 83(6): 1489– 1494.
- [5] Chun D L, Kim D Y. Microstructure evolution during the sintering of TiC-Mo-Ni cermets [J]. *J Am Cer Soc*, 1993, 76(8): 2049– 2052.
- [6] Yang J K, Lee H C. Microstructural evolution during the sintering of $\text{Ti}(\text{C}, \text{N})\text{-Mo}_2\text{C-Ni}$ alloy [J]. *Mater Sci & Eng A*, 1996, A209: 213– 217.
- [7] YU Lixin, LI Chenhui, XIONG Weihao, et al. Study of $\text{Ti}(\text{C}, \text{N})$ -based cermets manufactured by sinter-HIP [J]. *Cemented Carbide*, (in Chinese), 2001, 18(2): 69 – 73.
- [8] Lindau L, Stjernberg K G. Grain growth in TiC-Ni-Mo and TiC-Ni-W cemented carbides [J]. *Powder Metallurgy*, 1976, 19(3): 210– 213.
- [9] Fukuhara M, Mitani H. Mechanisms of grain growth in $\text{Ti}(\text{C}, \text{N})\text{-Ni}$ sintered alloys [J]. *Powder Metallurgy*, 1982, 25(1): 62– 68.
- [10] XIONG Weihao, HU Zhenhua, CUI Kun. Transitional layer of phase interfaces in $\text{Ti}(\text{C}, \text{N})$ -based cermet [J]. *Acta Metallurgica Sinica*, (in Chinese), 1996, 32(10): 1075– 1080.
- [11] LIU Ning, HUANG Ximing, ZHOU Jie, et al. The microstructure of $\text{Ti}(\text{C}, \text{N})$ based cermets [J]. *Journal of the Chinese Ceramic Society*, (in Chinese), 1999, 27(6): 750– 756.
- [12] LIU Ning, HU Zhenhua, CUI Kun, et al. Mechanical properties and microstructures of $\text{Ti}(\text{C}, \text{N})$ based cermets [J]. *Trans Nonferrous Met Soci China*, 1996, 6 (4): 117– 121.
- [13] Laoui T, Zhou H, Biest O V. Analytical electron microscopy of the core/rim structure in titanium carbonitride cermets [J]. *Int J RM & HM*, 1992, 11(4): 207 – 212.
- [14] Weast R C. *CRC Handbook of Chemistry and Physics* [M]. 70th Edition, Florida: CRC Press, 1989. F188 – 190.
- [15] LI Chenhui, XIONG Weihao, YU Lixin. Phase evolution of submicron $\text{Ti}(\text{C}, \text{N})$ base cermet [J]. *Rare Metals*, 2001, 20(4): 248– 254.
- [16] Andren H O. Microstructure development during sintering and heat treatment of cemented carbides and cermets [J]. *Mater Chem & Phys*, 2001, 67(3): 209– 213.

(Edited by HUANG Jin-song)